Supplemental Material

In-Plane Vibration of Hammerhead Resonators for Chemical Sensing Applications

Luke A. Beardslee[†,‡], Christopher Carron[†,§], Kemal S. Demirci[†,‖], Jonathan Lehman[†], Steven Schwartz[†,⊥,#], Isabelle Dufour[¶], Stephen M. Heinrich[∇], Fabien Josse[□], Oliver Brand*[†,#]

[†]School of Electrical and Computer Engineering, [⊥]School of Material Science and Engineering, and [#]Institute for Electronics and Nanotechnology, Georgia Institute of Technology, Atlanta, Georgia 30332, United States

[‡]Naval Submarine Medical Research Laboratory, Groton, Connecticut 06349-5900, United States

[§]Space and Intelligence Systems, Harris Corporation, Melbourne, Florida 32904, United States

[‖]Texas Instruments, Inc., Dallas, Texas 75243, United States

[¶]University of Bordeaux, IMS Lab, Talence 33400, France

[∇]Department of Civil, Construction and Environmental Engineering and [□]Department of Electrical and Computer Engineering, Marquette University, Milwaukee, Wisconsin 53201-1881, United States

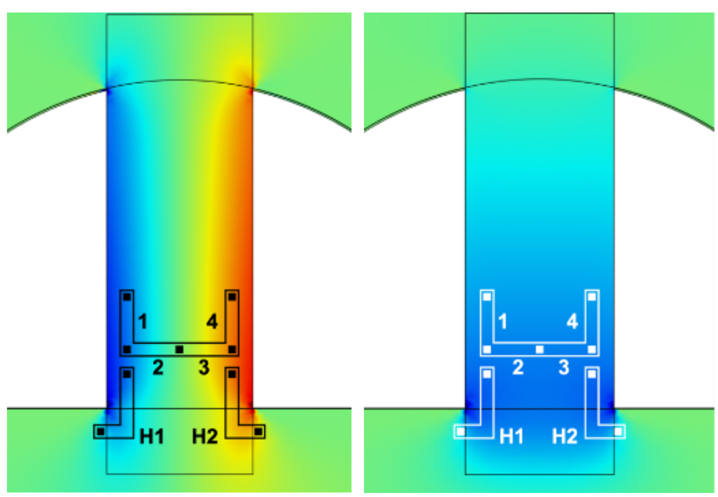

Figure S1. U-shaped Wheatstone bridge layout overlaid on the simulated stress distribution along the length direction of the cantilever stem of a F200A hammerhead resonator for the (left) fundamental in-plane and (right) fundamental out-of-plane resonance modes. Blue and red highlight compressive and tensile stresses, respectively, while green denotes near stress-free regions. The location of the heating resistors (H1 and H2), as well as the location of the four piezoresistors (1-4) arranged in a U-shaped Wheatstone bridge are shown.

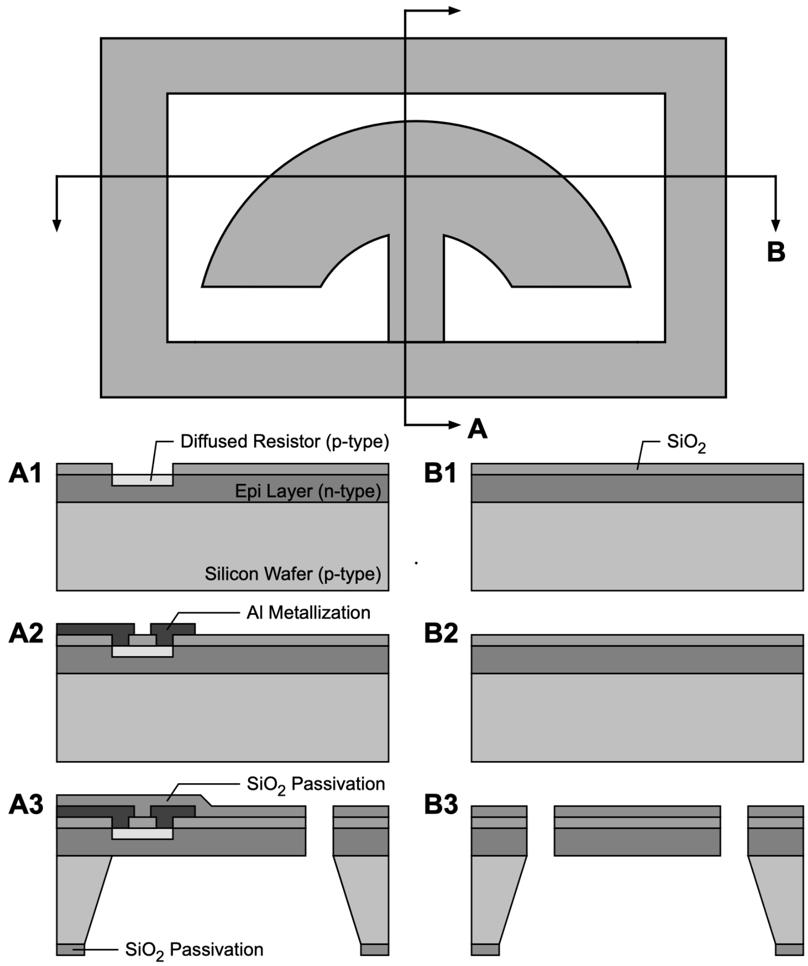

Figure S2. Schematic fabrication process for in-plane hammerhead resonators (adapted from [26]): (1) Diffused p-type resistor formation using solid-state diffusion sources and epi-wafer (SOI wafers can be used instead of epi-wafers). A silicon dioxide diffusion mask is patterned using inductively coupled plasma (ICP) etching to open diffusion windows. SUPREM simulations yield a junction depth of the piezoresistors of 1.2µm and a surface doping concentration of $3\text{-}4\times10^{18}$ cm^{-3} for the boron-doped piezoresistors. (2) Contact formation via photopatterning, ICP etching and aluminum metallization. The metallization can be performed either by e-beam evaporation or direct current (DC) sputtering. (3) Passivation deposition and etching, resonator release by KOH etching from the back of the wafer using an electrochemical etch stop (alternatively, DRIE (deep reactive ion etching) can be used with an etch stop on the buried oxide layer of the SOI wafer), and final microstructure release from the bulk micromachined membrane using DRIE from the topside. The recessed structure as shown in Figure S5 can be created by the addition of a passivation etch step followed by DRIE using a photoresist layer where only the head of the hammerhead is exposed. After the devices have been released, polymer sensing films can be selectively spray-coated onto the hammerhead by using a shadow mask. The shadow mask is drawn using computer aided design software, laser cut, then aligned by hand to the surface of the die. A fixture using hand screws can be used to secure the shadow mask in place during spray coating.

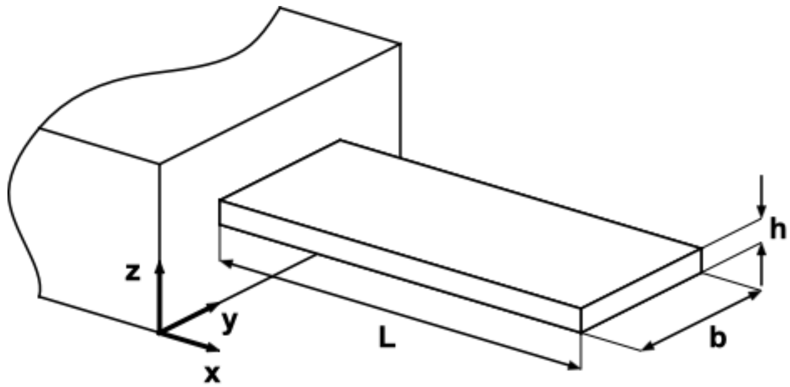

Figure S3. Schematic of prismatic cantilever beam with length L, width b, and thickness h.

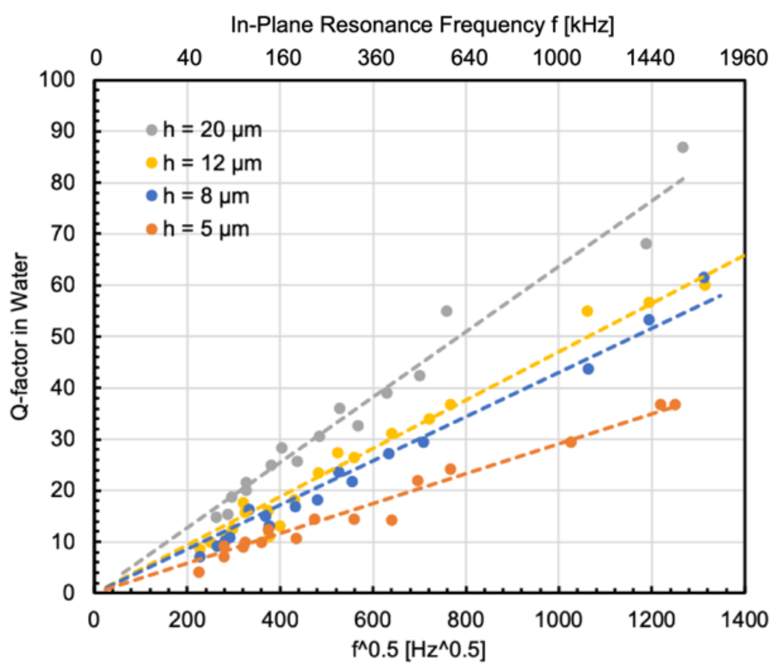

Figure S4. Measured Q-factor in water of prismatic beam cantilevers with various lateral dimensions and silicon thicknesses of 5, 8, 12 and 20 µm as a function of the square-root of the in-plane resonance frequency; the dashed lines represent linear fits through all data points of a respective thickness [23,32].

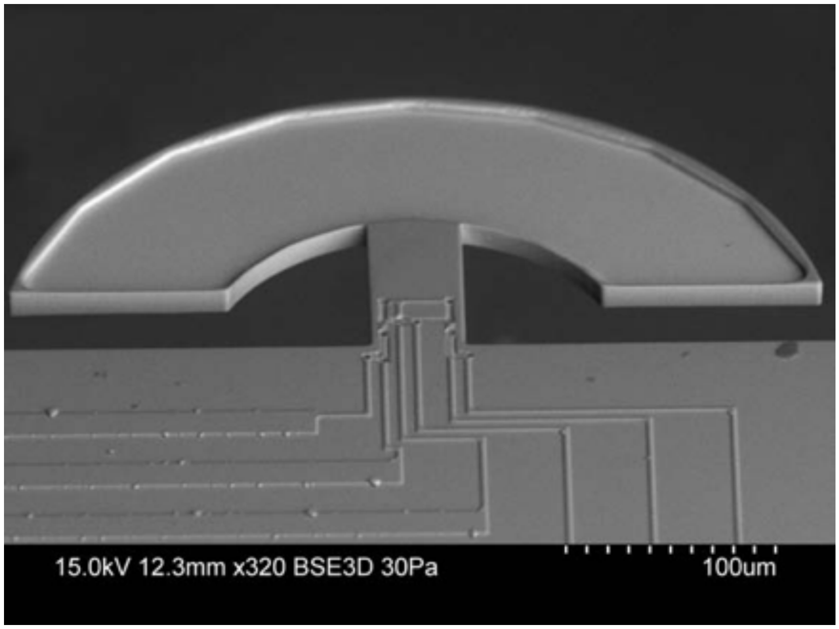

Figure S5. SEM micrograph of a F200A “bathtub” hammerhead device with a 45µm wide and 100µm long support cantilever and a semicircular annulus with an outer radius of 200µm. A recess has been etched into the hammerhead region to form a “bathtub” for sensing film deposition. None of the devices tested in this work were bathtub resonators.

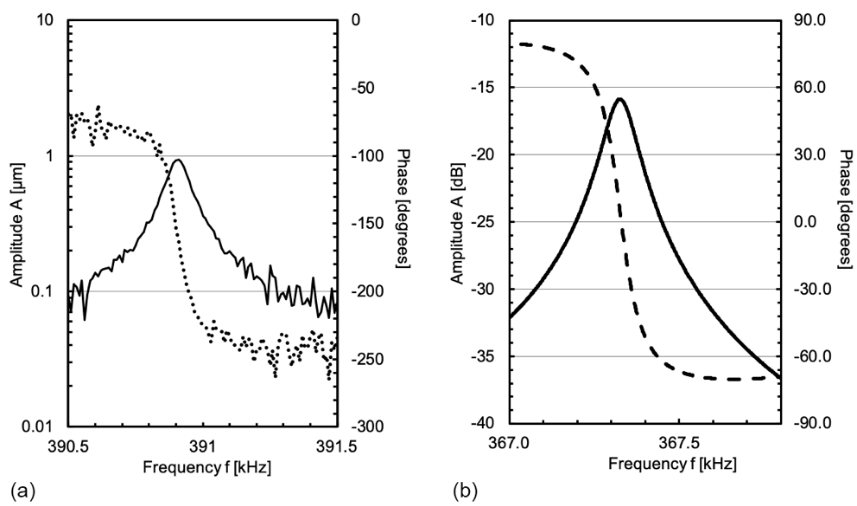

Figure S6. (a) In-plane vibration amplitude and phase -measured using Polytec MSA-500- of F200B resonator with 20 µm silicon thickness excited with V_{dc} = 2 V and V_{ac} = 2 V_p as a function of frequency around the in-plane resonance frequency; (b) Piezoresistive amplitude and phase transfer characteristic of F200B resonator with 20 µm silicon thickness as a function of frequency around the in-plane resonance mode.

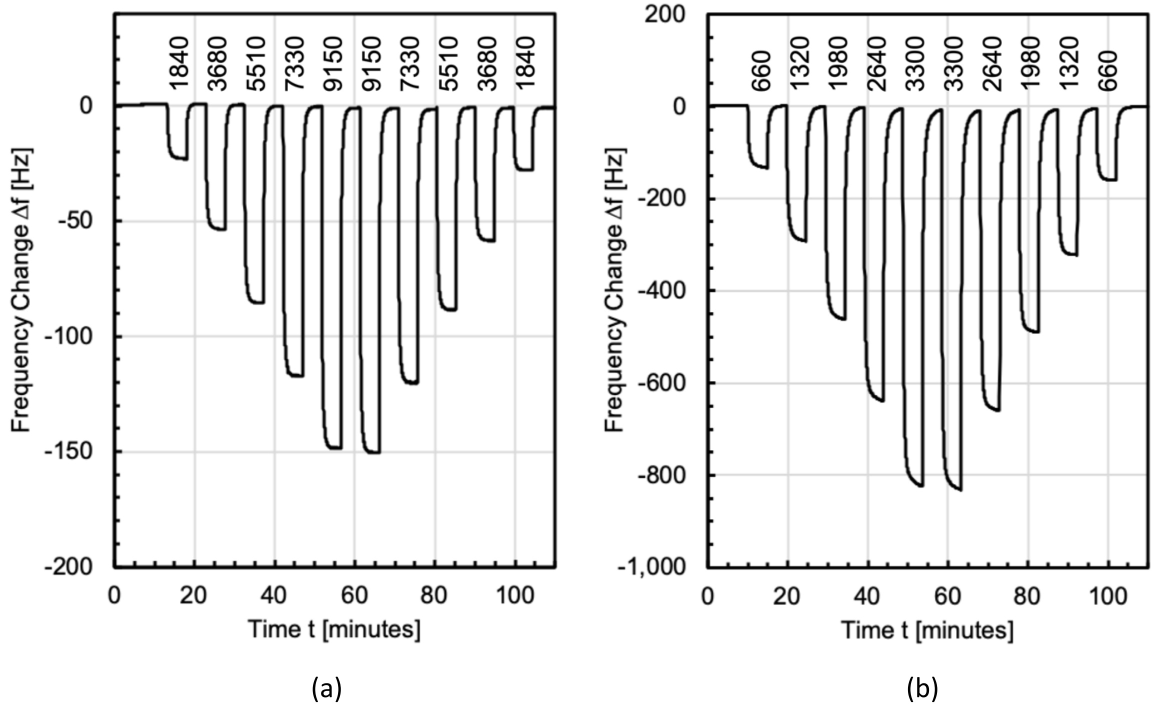

Figure S7. Sample gas measurement exposing a F200A hammerhead resonator (20μm silicon thickness) coated with 1.5 μm poly(isobutylene) (PIB) to different (a) benzene and (b) m-xylene concentrations. Analyte concentrations in ppm are shown in the graph.

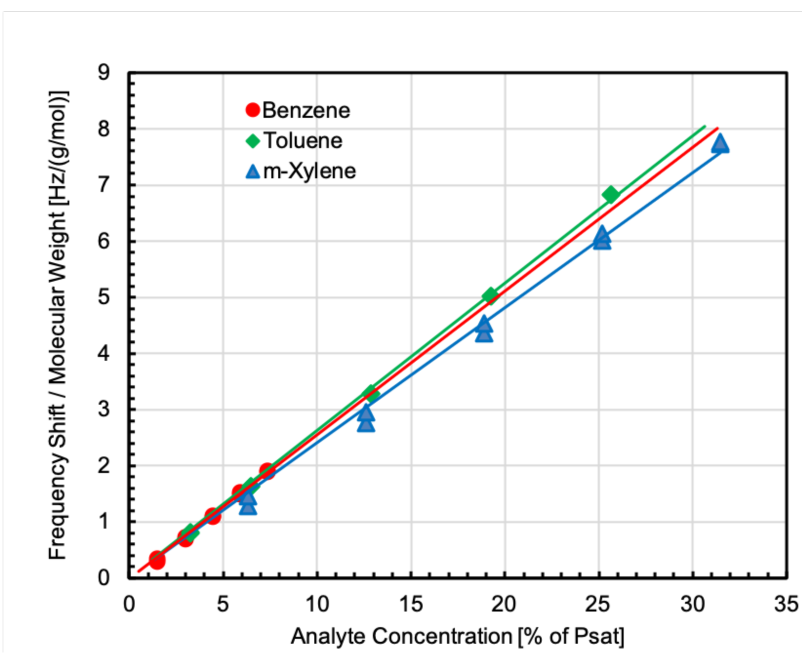

Figure S8. Normalized sensitivity curves showing the absolute value of the measured steady-state frequency change divided by the analyte' molecular weight for the F200A hammerhead resonator coated with 1.5μm PIB as a function of the m-xylene, toluene and benzene concentrations in percent of their room-temperature saturated vapor pressure.

Table S1. Comparison of Q-factor of fundamental in-plane mode of hammerhead and prismatic beam resonators with 8µm and 20 µm silicon thicknesses. The data are extracted from either optical or purely electrical measurements. The 8 µm thick F150B resonator had a 300nm thick gold layer on its head region which may have lowered its Q (besides lowering its resonance frequency). Please see Figure 2 in the text for details about the device structure and nomenclature for the hammerhead resonators. Briefly, the designation F200B means a hammerhead resonator with a 200 µm radius head (and a wider hammer design, which has only a small gap between the support beam and the head of the resonator. Conversely, the designation F150A corresponds to a hammerhead with a radius of 150 µm and a narrower head design with a larger gap between the resonator head and the support beam. The prismatic beams are denoted by their width and length, i.e. 45W600L refers to a 45 µm wide and 600 µm long cantilever beam.

	45W400L	F200B	60W400L	90W400L	F150B	F150A	45W200L
Si Thickness [µm]	20	20	20	20	20	20	20
f_{ip} [kHz]	349.4	390.9	437.0	636.8	796.8	840.0	1,254.9
Q_{ip}	3,167	4,850	2,983	2,533	5,107	4,489	3,160
Measurement	optical	optical	electrical	optical	optical	electrical	electrical
Si Thickness [µm]	8	8	8	8	8	8	8
f_{ip} [kHz]	336.4	386.3	431.8	–	704.4	818.4	1,212.0
Q_{ip}	1,654	3,138	2,353	–	2,326	3,836	2,140
Measurement	electrical	optical	electrical	–	electrical	electrical	electrical